



Effect of CuAl_2 on the Microstructure and Hardness of Al-Si-xCu Alloys Produced by Powder Metallurgy

Shakib Alsowidy^{1,*}, Mohammed S. Gumaan², Olfat Humaid^{1,3,*} and Belqueis Al-Asry¹

¹Department of Physics, Faculty of Science, Sana'a University, Sana'a, Yemen.

²Biomedical Engineering Department, Faculty of Engineering, University of Scienc & Technology, Sana'a, Yemen.

³Department of Physics, Faculty of Applied Science, Hajjah University, Hajjah, Yemen.

*Corresponding author: sh.alsowidy@su.edu.ye and o.humaid1234@gmail.com

ARTICLE INFO

Article history:

Received: Oct 19, 2023

Accepted: Nov 8, 2023

Published: Nov, 2023

KEYWORDS

1. Hypereutectic
2. Microstructure
3. XRD
4. Al-Si alloy
5. Vickers hardness.

ABSTRACT

Aluminum alloys are important in many industrial applications because of their light weight and good mechanical properties. In this study, the effect of copper addition with different percentages (0, 0.1, 0.2, 0.3wt. %) on the microstructure and mechanical strength of Al-Si alloy were studied using X-ray fluorescence (XRF), X-ray diffraction (XRD), scanning electron microscope (SEM) and Vickers hardness (Hv) tests. XRD and SEM analyses showed that the Al-Si alloy consisted of α -Al and Si phases. The intermetallic compound (IMC) CuAl_2 was detected with the addition of Cu. This IMC causes a change in the lattice constant and inter-atomic spacing (d_{hkl}). The distortion and dense of the microstructure are considered indications of the enhancement in the hardness of alloys. The Vickers hardness (Hv) was measured for the samples before and after sintering. The highest value was 28.755 Hv with 0.2wt. % Cu after sintering, whereas the smallest value was 11.643 Hv without Cu content before sintering. This improvement in hardness is attributed to the temperature that promotes the diffusion of Cu atoms into the Al lattices.

CONTENTS

1. Introduction
2. Related Work
3. Discussion And Results
4. Methodology
5. Conclusion And Future Work
6. References

1. Introduction:

Aluminum alloys are important materials in many industrial and structural applications. This is due to their light weight and good mechanical properties. Aluminum and its alloys are currently the most suitable structural materials. Many studies have recently been conducted and concentrated on aluminum alloys to improve new

Al alloys that are stronger, ductile, corrosion resistant, and have a large strength–weight ratio [1-7]. In previous studies, Pure aluminum was alloyed with various alloying elements to achieve the desired properties. The major alloying elements are Cu, Mn, Zn, and Si [8]. For economic and environmental requirements, and due to its high S/W ratio, high wear resistance,

and excellent corrosion resistance, compacted powder Al-Si alloys have been commercially used in the automotive industry, particularly in the car's structure, cylinder heads, cylinder blocks, pistons and valve lifters and engine block [9-13]. The mechanical properties primarily depend on the heat-treatment conditions and the presence of other elements in the matrix aluminum alloy [14,15]. Different elements such as carbon (C), zinc (Zn), lead (Pb), tin (Sn), indium (In), cadmium (Cd), magnesium (Mg), copper (Cu), ferum (Fe), beryllium (Be), manganese (Mn), chromium (Cr), and nickel (Ni) are alloyed to Al-Si alloys to further enhance their properties [16]. Powder metallurgy (PM) is a highly developed method for manufacturing and producing reliable materials, especially structural materials [17,18].

According to the PM method, the mixture powder is compacted with a large hydraulic pressure to produce sheet or disk samples. In this study, disk samples of Al-Si-xCu alloys were produced using the PM technique. This work aims to investigate the influence of various concentrations of copper atoms on the mechanical hardness and microstructure of sintered Al-Si-xCu alloys prepared by the powder metallurgy method.

1. Materials and Methods

As a basis for all experiments, alloys (Al-Si-xCu) with varying Cu percentages ($x = 0, 0.1, 0.2, 0.3$ wt. %) denoted in this study as A, B, C, and D respectively, were prepared from Al, Si, and Cu with a high purity of (99.99%). Each metal powder was weighed in a sensitive electric balance with an accuracy of approximately 1×10^{-4} gm to obtain the required composition, as shown in Table (1). The balanced elements were mixed in powder form at room temperature. A mixing time was 3 min to obtain a homogeneous distribution. After mixing, the powder was compacted at 250KN into cylindrical disks under a hydraulic pressure system for 5 min to ensure consistency. Compacted cylindrical disks were obtained with dimensions of 32 mm in diameter and 6 mm in thickness, as shown in Figure. 1..

Table 1: The balanced elements were mixed in powder form at room temperature

Chemical compositions (wt. %)			
Samples	Al	Si	Cu
A1	Balance	17	0
A2	Balance	17	0.1
A3	Balance	17	0.2
A4	Balance	17	0.3

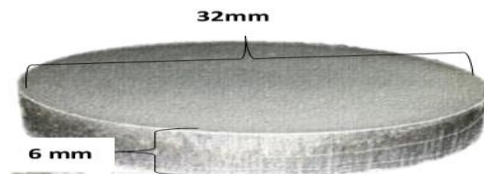


Figure. 1: Compressed sample.

The compact stage was followed by another stage known as the sintering process, where the compressed samples were placed in a graphite crucible using an electric furnace at approximately 450°C with a cooling rate (0.04 °C /s) for 3 h, which increased the bonding of particles. For X-ray diffraction (XRD) analysis, a Shimadzu X-ray diffractometer (EDX-720) with Cu k_{α} radiation ($\lambda = 1.54056 \text{ \AA}$) was used to determine the alloy phases and identify other lattice parameters. Microstructure analysis was carried out on a scanning electron microscope (SEM) (JEOL JSM-6510LV, Japan) operate at 30Kv with a high resolution of 3 nm. The Vickers hardness test (localized plastic deformation resistance or impact force resistance) was performed using mechanical equipment, as shown in Figure.2.

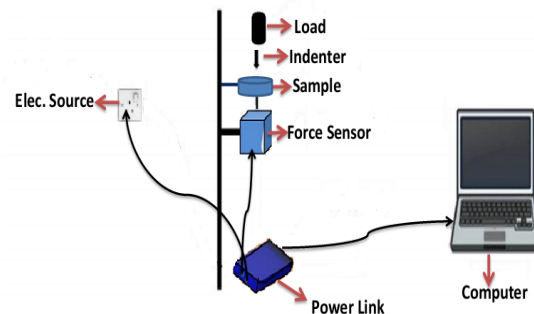


Figure. 2: Schematic diagram of Vickers hardness tester.

3. Results and Discussion

3.1 Microstructure Analysis

3.1.1 X-Ray Fluorescence (XRF)

The following Table (2) shows the weight percentage of different elements present in the prepared Al-Si-xCu samples using X-ray Fluorescence technique.

Table 2: Weight percentage of different elements present in Al-Si-xCu alloy.

Elements (wt.%)	Alloys			
	A1	A2	A3	A4
Al	82.19	82.66	81.23	81.94
Si	16.64	16.89	17.97	17.09
Cu	0.024	0.089	0.221	0.385
Zn	0.016	0.017	0.028	0.03
Zr	-----	-----	0.002	0.002
Mo	0.002	0.002	0.003	0.004
Sn	-----	-----	0.003	-----
Pb	0.013	0.014	0.021	0.023

3.1.2 X-Ray Diffraction (XRD)

X-ray diffraction patterns of Al-Si-xCu ($x=0 - 0.3$ wt. %) are shown in Figure. (3). From Figure. (3a), there are two original phases: α -Al (Fcc) and Si (Fcc). Lines (111, 200, and 220) represent the Al phase and lines (111, 220, 311, and 400) represent the Si phase. This result is in good agreement with the literature [19] and standard powder diffraction data (PDF), as shown in Table (3). This observation was verified by SEM, as discusses in the next section.

According to the standard powder diffraction data (PDF), the fingerprints of the Al and Si phases are very clear before and after the addition of Cu.

From Figure. (3), a new phase was detected with lines (211, 112, 222, 411, and 402). According to the Al-Cu phase diagram [20] and previous literature [21], this intermetallic compound (IMC) is CuAl_2 .

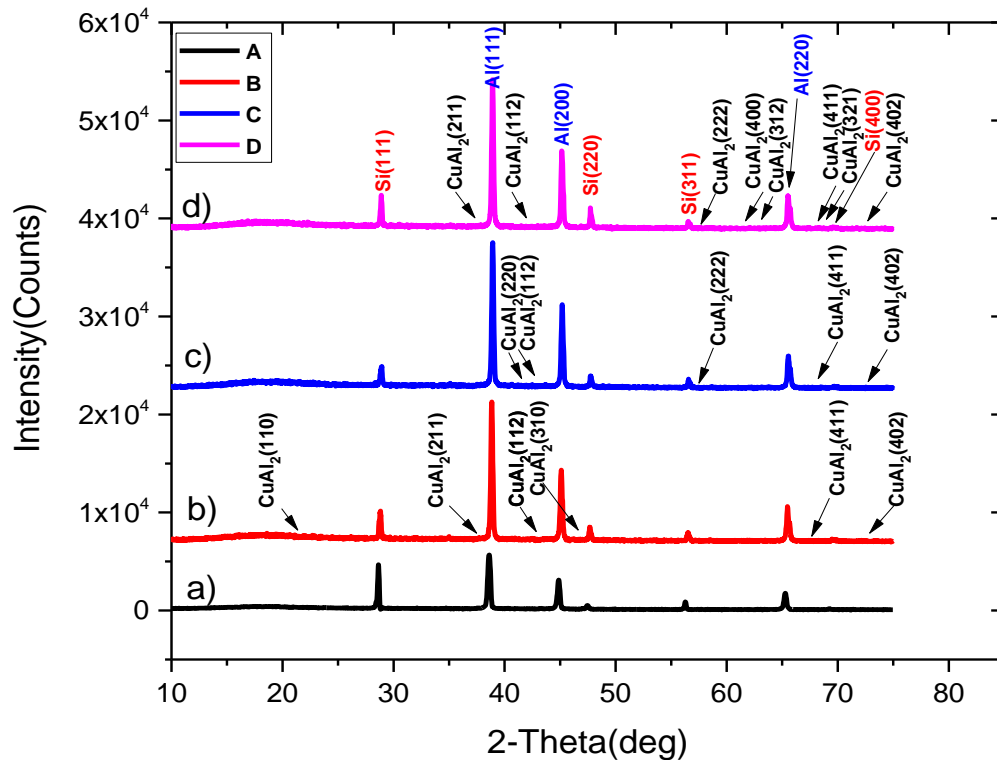


Figure. 3: The XRD patterns of Al-Si-xCu alloys.

Table 3: Phases and (JCPDS-ICDD) references Al-Si-xCu alloy.

phases	A1		A2			A3			A4		
	Al	Si	Al	Si	CuAl ₂	Al	Si	CuAl ₂	Al	Si	CuAl ₂
(JCPDS- ICDD) Reference	PDF# 04-0787	PDF# 27-1402	PDF# 04-0787	PDF# 27-1402	PDF# 25-0012	PDF# 04-0787	PDF# 27-1402	PDF# 25-0012	PDF# 04-0787	PDF# 27-1402	PDF# 25-0012

The Figure. (3) was indexed and the expected data of intensity and full width at half maximum (FWHM) were tabulated, as shown in Table (4), respectively. When comparing the Al peaks before and after Cu addition, it can be seen that the peak intensity increases and the FWHM decreases with increasing Cu content for all lines, as shown in Table (4). In addition, there was a small shift in the peak position to a high angle with increasing Cu content, as shown in Table (4).

Table 4: Intensity, FWHM and 2θ(deg) of Al lines for all samples.

Lines	Samples	Intensity	FWHM	2θ(deg)
111	A1	5463	0.278	38.6
	A2	10067	0.197	38.82
	A3	10684	0.186	38.9
	A4	10863	0.189	38.899
200	A1	2953	0.27	44.879
	A2	5389	0.202	45.08
	A3	6211	0.193	45.16
	A4	6033	0.189	45.14
220	A1	1674	0.277	65.28
	A2	2652	0.187	65.461
	A3	2822	0.221	65.54
	A4	2911	0.217	65.521

Even when this shift in the angle position is less than 0.3°, this shift and mismatching in the angle position reflects its-self in the incoincide of interplanar spacing (d_{hkl}) levels before and after Cu addition, as confirmed by the values in Table (5). This inconsistent in the (d_{hkl}) levels is associated with lattice defects, localized the strain deformation and the change in lattice

parameters of the Al lattice, as confirmed by the values in Table (5).

Table 5: Interplanar spacing, lattice constant and Micro-strain of Al lines for all samples.

Lines	Samples	d _{hkl} (Å)	Lattice	Micro-
111	A1	2.3305	4.0365	3.46
	A2	2.3178	4.0145	2.44
	A3	2.3132	4.0066	2.30
	A4	2.3133	4.0068	2.33
200	A1	2.018	4.036	2.85
	A2	2.0095	4.019	2.12
	A3	2.0061	4.0122	2.02
	A4	2.0069	4.0138	1.98
220	A1	1.4281	4.0393	1.89
	A2	1.4246	4.0294	1.27
	A3	1.4231	4.0251	1.50
	A4	1.4235	4.0263	1.47

According to a previous study [22], when strange atoms are added to the material lattice, they may diffuse and dissolve in the lattice and finally lift in defects and localized deformation. In this investigation, the diffusion of copper atoms into Al lattices was expected owing to the sintering process. This diffusion increases with increasing temperature. This process explains the changes in lattice constants and inter-atomic spacing (d_{hkl}) before and after Cu addition and the enhancement in hardness, as shown in Table (5).

According to the Scherrer formula [23], the particle size in the crystallographic direction for all alloys was calculated and is tabulated in Table (6).

$$D=0.9\lambda/\beta\text{Cos}\theta \quad (1)$$

where β is the broadening of the diffraction line measured at half its maximum intensity (radians), D is the crystallite size, θ is the Bragg angle and λ is the X-raywavelength.It can be seen from Table(6) that the grains for all lines after Cu addition were larger than before. This is further evidence for the diffusion of Cu atoms intoAl lattices. In addition,Poisson's ratio provides a significant interpretation of the behavior of particle size with various orientations (111), (200), and (220).

Poisson's ratio is the ratio of transverse strain to the equivalent axial strain on a material under

axial stress [24]. This increase reflected its-self in the whole grains of the alloys, as confirmed in Table (6).

The dislocation density (δ) represents the number of defects in the sample and defined as the length of dislocation lines per unit volume of the crystal. This dislocation density is calculated using the following equation [25]:

$$\delta = \frac{1}{D^2} \quad (2)$$

where (D) the average crystallite size. The inverse relationship between δ and D is shown in Figure. (4), and Table (6).

Table 6: Particle size and dislocation density of Al-Si-xCu alloys.

Alloys	Lines	particle		Dislocation
A1	111	30.282	32.060	97.285
	200	31.837		
	220	34.062		
A2	111	42.761	45.285	48.763
	200	42.586		
	220	50.507		
A3	111	45.302	44.214	51.094
	200	44.585		
	220	42.756		
A4	111	44.582	44.549	50.388
	200	45.525		
	220	43.539		

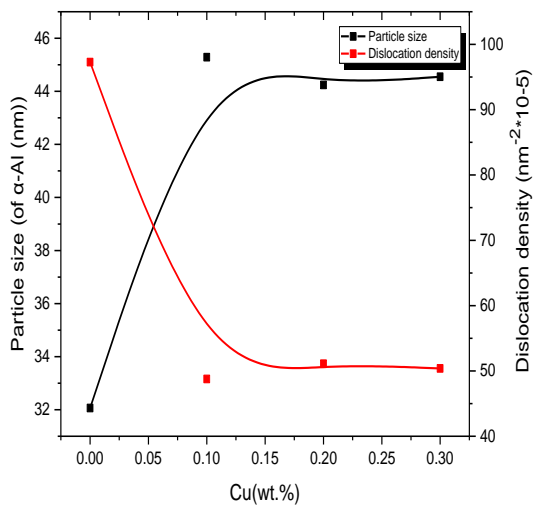
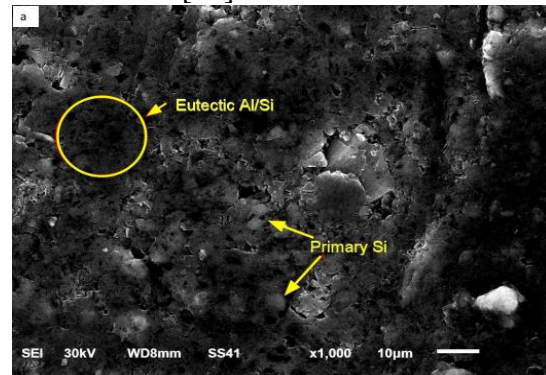


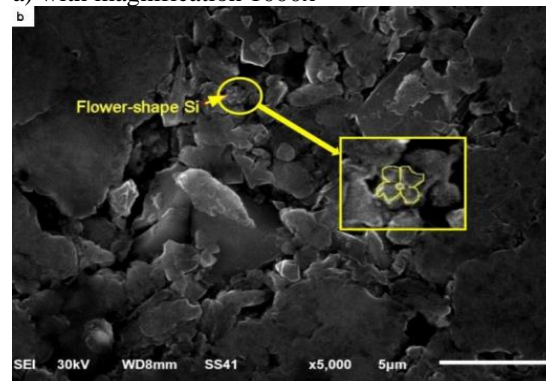
Figure 4: Particle size and dislocation density as a function of Cu addition.

3.1.3 Scanning Electron Microscope (SEM)

Figures. (5) - (7) show SEM images of the samples surfaces after sintering. The surfaces of the samples were scanned using secondary electron beam type1 (SE1) with an accelerated voltage of 30 KV and various magnifications. The influence of the Cu-content on the internal structure of the compacted alloys is also observed in the same Figures. Based on a previous study [26] and Figure. (5), it can be observed that the microstructure of the Al-Si alloy consists of primary crystalline silicon and an Al-Si eutectic phase surrounded by a dendritic primary α -Al phase with a higher size and volume fraction. The silicon particles were found to be spherical and flower-shaped, as shown in Figure. (5a). In addition, the flower-like shape of Si is clearly observed in Figure. (5b) at a magnification of 5000x and confirmed with Benson result [27].



a) with magnification 1000x



b) with magnification 5000x.

Figure. 5: SEM images of Al1 alloy.

With the addition of copper atoms and sintering temperature, the diffusion of copper atoms increased as the copper atoms concentration increased. This diffusion increases the aluminum dendrite arms, especially the secondary dendrite arms (SDA) [26], as shown in Figure. (6a). In addition, the dendritic nature of the aluminum particles is very clear, as can be seen from the image in Figure. (6b), which was processed and modified using ImageJ software.

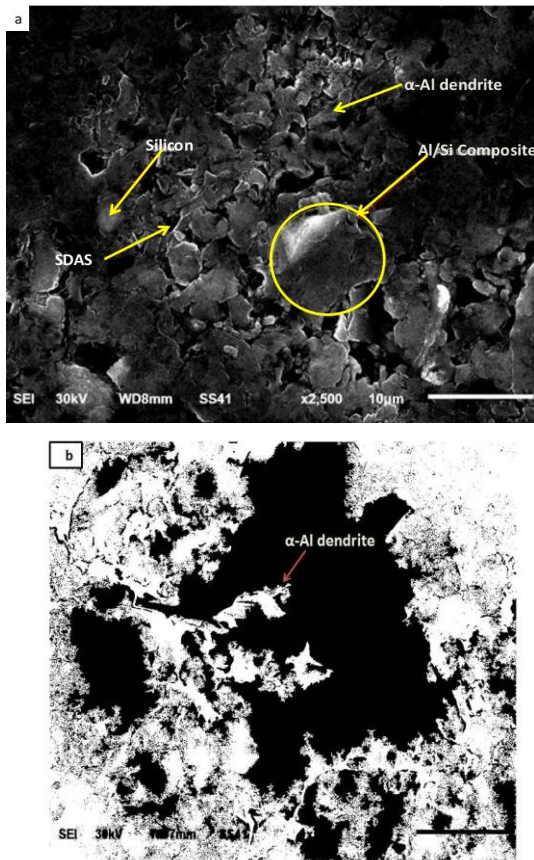
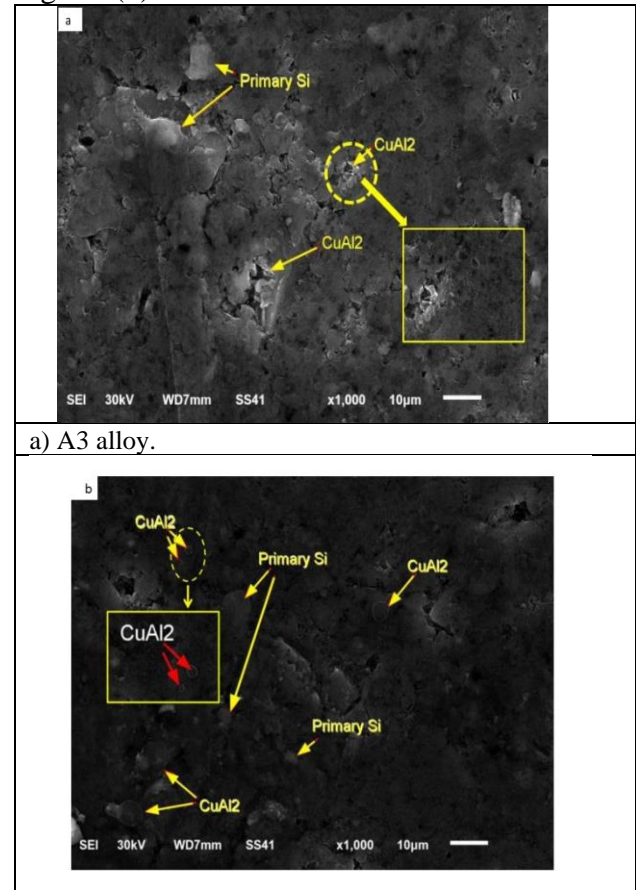


Figure. 6: SEM images of A2 alloy.

4. Discussion

Addition 0.2wt.% of Cu leads to increase the size of primary Si and to precipitate the CuAl₂ IMC as fibers structure as shown in Figure. (7a) while the addition 0.3Wt. % of Cu leads to form CuAl₂IMC as bubbles structure distributed in whole structure, as shown in Figure. (7b). The changes in the microstructure mentioned above are attributed to the copper atoms and sintering process, and all these changes reflect in the

enhancement of the localized plastic deformation (Hv) on the surfaces of the samples, as shown in Figure. (8).



a) A3 alloy.

b) A4 alloy

Figure 7: SEM images

a) A3 alloy
b) A4 alloy.

3.2 Vickers Hardness Measurements

In mechanical design, the mechanical properties required to know and specify the materials are stiffness, toughness, and localized plastic deformation (hardness). The hardness of a material is an important mechanical property, particularly in structural applications. Vickers hardness was determined before and after the sintering process using the following formula [28]:

$$H = 1.85 \frac{L}{d^2} \tag{3}$$

where L is the indentation load (kg) and d is the mean diagonal of the indentation (mm).

Table (7) and Figure. (8) presents the Vickers hardness results. It is clear that (i) the higher the

copper content in the alloy, the higher the hardness value. This agrees with the findings of Zeren et al. [29], and (ii) the Vickers hardness after the sintering process was higher than that before sintering. This increase was explained by Ciolek et al. [30]. They reported that the most visible increase in hardness was obtained when the samples were sintered, which enabled the generation of the highest number of finely dispersed particles in the aluminum matrix by diffusion. Furthermore, this investigation showed that the addition of Cu in various amounts considerably increased the volume fractions of the intermetallic compounds, as shown in the XRD and SEM images. Therefore, this variation in the volume fraction of IMC reflects the hardness values, as shown in Table (7) and Figure. (8).

Table 7: Vickers Hardness Number of Al-Si-xCu.

Alloys	Vickers Hardness (Hv)	
	Before	After Sintering
A1	11.643	13.1317
A2	12.735	13.657
A3	14.7696	28.755
A4	27.439	18.153

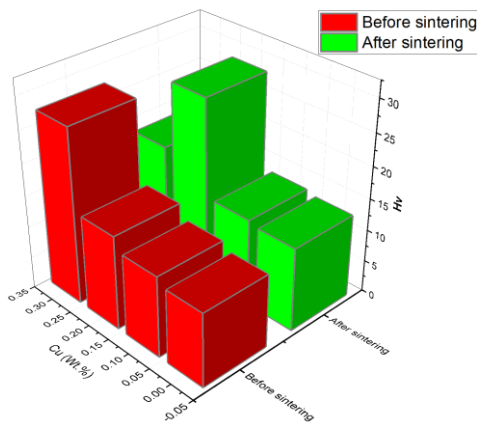


Figure. 8: Vickers hardness as a function Cu content.

5. Conclusion

The effect of Cu on the microstructure and mechanical properties (hardness) of the Al-Si-xCu alloys was investigated. The microstructure

of the Al-Si alloy, as observed through scanning electron microscope (SEM), was found to consist of primary crystalline silicon and an Al-Si eutectic phase surrounded by a dendritic primary α -Al phase with a higher size and volume fraction. While the addition of Cu as an alloying element, leads to the formation of intermetallic compounds CuAl_2 , which strengthens the Al-Si alloy. The formation of CuAl_2 precipitates promoted an increase in hardness from 11.643 Hv in the binary Al-Si to 27.439 Hv in the ternary Al-Si-0.3wt.%Cu. This phase impeded the movement of dislocations and, as a result, the alloy exhibited high hardness. However, the highest value of 28.755 Hv was achieved with an addition of 0.2wt. % Cu after sintering. This is attributed to the temperature promoting diffusion of copper atoms into the Al lattices, which improves the hardness.

5. References

- [1] Karakoşse, E.; Keskin, M. Structural Investigations of Mechanical Properties of Al Based Rapidly Solidified Alloys. *Material and Design* **2011**, 32, 4970-4979. <https://doi:10.1016/j.matdes.2011.05.042>
- [2] Krishnan, P. K. et al. Production of Aluminum Alloy-Based Metal Matrix Composites Using Scrap Aluminum Alloy and Waste Materials. Influence on Microstructure and Mechanical properties. *Journal of Alloys and Compounds* **2019**, 784, 1047–1061. <https://doi:10.1016/j.jallcom.2019.01.115>.
- [3] Bardi, F.; Cabibbo, M.; Evangelista, E.; Spigarelli, S.; Vukcevic, M. An Analysis of Hot Deformation of an Al-Cu-Mg Alloy Produced by Powder Metallurgy. *Material Science and Engineering: A* **2003**, 339 (1-2), 43-52. [https://doi:10.1016/S0921-5093\(02\)00103-X](https://doi:10.1016/S0921-5093(02)00103-X)
- [4] Kumar, S.; Balasubramanian, V. Effect of Reinforcement Size and Volume Fraction on the Abrasive Wear Behaviour of AA7075 Al/SiCp P/M Composites. *Tribology International* **2010**, 43, 414-422. <https://doi:10.1016/j.triboint.2009.07.003>
- [5] Yamanoglu, R.; Zeren, M.; German, R. M. Solidification Characteristic of Atomized AlCu4g1-SiC Composite Powder. *Journal of Mining and Metallurgy Section.B* **2012**, 48(1), 73–79. <https://doi:10.2298/jmmb110717005Y>.

- [6] Zor, S.; Zeren, M.; Ozkazanc, H.; Karakulak, E. Effect of Cu on the Corrosion of Al-Si Eutectic Alloys in Acidic Solutions. *Anti-Corrosion Methods and Materials* **2010**, *57*, 185–191. <https://doi:1108/00035591011058192>.
- [7] Rosliza, R.; Wan Nik, W. B.; Senin, H. B. The Effect of Inhibitor on the Corrosion of Aluminum Alloys in Acidic Solutions. *Material Chemistry and Physics* **2008**, *107*, 281–288. <https://doi:10.16/j.matchemphys.2007.07.013>.
- [8] Barrirero J. Eutectic Modification of Al-Si casting alloys. **2019**. <https://doi:/10.22028/D291>
- [9] Warmuzek, M. Introduction to Aluminum–Silicon Casting Alloys. International, Materials Park, Ohio, USA, **2004**, 2(1-9). www.asminternational.org.
- [10] Kotadia, H.R.; Hari Babu, N.; Zhang, H.; Fan, Z. Microstructural Refinement of Al–10.2%Si Alloy by Intensive Shearing. *Materials Letters* **2010**, *64*(6), 671–673. <https://doi.org/10.1016/j.matlet.2009.12.03>
- [11] Taylor, J.A.; Couper, M.J.; Smith, C.L.; Singh D.P.K. Dissolution, Recovery and Fade of Sr Master Alloys in Al-7Si-0.5Mg Casting Alloy. *Light Metals, The Minerals, Metals and Materials Society* **2005**, 1095–1100. <https://espace.library.uq.edu.au/view/UQ:102706>
- [12] Liao, H.; Sun, Y.; Sun, G. Correlation Between Mechanical Properties and Amount of Dendritic α -Al Phase in as-Cast near-Eutectic Al-11.6%Si Alloys Modified with Strontium. *Materials Science and Engineering: A* **2002**, *335*(1-2), 62–6. [https://doi:10.1016/S0921-5093\(01\)01949-9](https://doi:10.1016/S0921-5093(01)01949-9)
- [13] Lasa, L.; Rodrigues-Ibade, J. M. Wear Behaviour of Eutectic and Hypereutectic Al-Si-Cu-Mg Casting Alloys Tested Against a Composite Brake Pad. *Materials Science and Engineering: A* **2003**, *363*(1-2), 193–202. [https://doi:10.1016/S0921-5093\(03\)00633-6](https://doi:10.1016/S0921-5093(03)00633-6)
- [14] Polmear, I.J. *Light Alloys from Traditional Alloys to Nanocrystals*. 4thed., Elsevier-Butterworth Heinemann, **2006**. <https://books.google.com>
- [15] Altshuller, B. *Aluminum Brazing Handbook*, 4th ed., The Aluminum Association, Inc, **1990**. <https://www.aluminum.org/aluminum-brazing-handbook>.
- [16] Ervina Efzan, M.N.; Kong, H. J.; Kok C. K. Effect of Alloying Element on Al-Si Alloys: A Review **2013**, *845*, 355–359. <https://doi:10.4028/www.scientific.net/MR.845.355>
- [17] Panda, A. et al. Advantages and Effectiveness of the Powder Metallurgy in Manufacturing Technologies. *Metallurgical* **2018**, *57* (4), 353–356. <https://www.google.com>
- [18] Araoyinbo, A.O.; Ishola F.A.; Salawu E.Y.; Biodun, M.B.; Samuel, A.U. Overview of Powder Metallurgy Process and its Advantages **2022**. <https://doi.org/10.1063/5.0092502>.
- [19] Santos, S.; Toloczko, F.; Merij, A.; Saito, N.; Silva, D. Investigation and Nanomechanical Behavior of the Microconstituents of Al-Si-Cu alloy After Solution and Ageing Heat Treatments. *Materials Research* **2021**, *24*(2). <https://doi.org/10.1590/1980-5373-MR-2020-0329>
- [20] Massalski, T.B., Murray, J.L., Bennett, L.H., Baker, H. American Society for Metals. Binary Alloy Phase Diagrams. Metals Park (OH), American Society for Metals **1986**, *1*, 2224. <https://www.world.org>.
- [21] S.An, M.kim, Ch.Huh and Ch.Kim, "Microstructure and Mechanical Property of Al₆Si₂Cu Alloy Subjected to Double-Solution Heat Treatment, *Metals* **2022**, *12*(1), 18. <https://doi.org/10.3390/met12010018>
- [22] Khorsand Zak, A.; Abd Majid, W.H.; Abrishami, M. E., Ramin, Y. *Solid State Sciences* **2011**, *13*, 251–256. <https://www.sciencedirect.com>
- [23] Patterson, A. The Scherrer Formula for X-Ray Particle Size Determination. *Physical Review* **1939**, *56*(10), 978–982. <https://doi.org/10.1103/phys.Rev.56.978.1939>
- [24] Ford, H. *Materials Science and Engineering*. **1974**, *14*(1). <https://anupturnedworld.files.wordpress.com/2016/06/callister-materials-science-and-engineering.pdf>
- [25] Dhanam, M.; Prabhu, R. R.; Manoj P. K. Investigations of Chemical Bath Deposited Cadmium Selenide Thin Films. *Materials chemistry and physics* **2008**, *107*, 289–296. <https://doi:10.1016/j.matchemphys.2007.07.011>
- [26] Afanasyev, V. K.; Popova, M. V.; Malyukh, M. A.; Prudnikov, A. N. Features of Structure Formation and Thermal Expansion of High Alloys of the Al–Si –Cu System. *Materials Science and Engineering* **2020**, *866*. <https://doi:10.1088/1757-899X/866/1/012035>
- [27] Njuguna, B; yan Li, J.; Tan, Y.; qian Sun, Q.; ting Li, P. Grain Refinement of Primary Silicon in Hypereutectic Al-Si Alloys by Different P-Containing Compounds. *Research and Development* **2021**, *18*(1), 37–44. <https://doi.org/10.1007/s41230-021-0074-2>
- [28] Krishna, S.; Karthik, M. Evaluation of Hardness Strength of Aluminium Alloy (AA6061) Reinforced With Silicon Carbide. *International J.Recent Technology*

Mechanical Electronic Engineering **2014**, 1(4), 14–18.

<http://www.ijrmee.org/download/1428305064.pdf>.

- [29] Zeren, M.; Karakulak, E. Study on Hardness and Microstructural Characteristics of Sand Cast Al–Si–Cu Alloys. *Bulletin of Materials Science* **2009**, 32(6), 617-620.

<https://link.springer.com/article/10.1007/s12034-009-0095-8>

- [30] Ciołek, Y.; Jo'Z'Wiak, S.; Karc Zewski, K." Possibility of Strengthening Aluminum Using Low-Symmetry Phases of the Fe-Al Binary System. *Metallurgical and Materials Transaction:A* **2019**, 50(4), 1914-1921.

<https://doi.org/10.1007/s11661-019-05110-6>.